Background Parenchymal Signal Enhancement Ratio at Preoperative MR Imaging: Association with Subsequent Local Recurrence in Patients with Ductal Carcinoma in Situ after Breast Conservation Surgery[1]

Sun-Ah Kim, MD
Nariya Cho, MD
Eun Bi Ryu, MD
Mirinae Seo, MD
Min Sun Bae, MD
Jung Min Chang, MD
Woo Kyung Moon, MD

Purpose: To retrospectively investigate whether the background parenchymal features around a tumor at preoperative dynamic contrast material–enhanced magnetic resonance (MR) imaging are associated with ipsilateral breast tumor recurrence (IBTR)–free survival in patients with ductal carcinoma in situ (DCIS) after breast conservation surgery.

Materials and Methods: The institutional review board approved this study, and the requirement for informed consent was waived. Between 2004 and 2009, 215 consecutive women with pure DCIS who had undergone preoperative dynamic contrast-enhanced MR imaging and curative breast conservation surgery were identified. Clinical-pathologic features (age, menopausal status, presentation of clinical findings, biopsy method, tumor size, nuclear grade, hormonal receptor status, margin status, and adjuvant therapy) and MR imaging features (lesion size, background parenchymal enhancement grade, fibroglandular density, parenchymal signal enhancement ratio [SER] around the tumor, lesion type, and lesion kinetics) were analyzed. A Cox proportional hazards model was used to determine the association between MR imaging variables and IBTR-free survival after controlling for clinical-pathologic variables. Reproducibility of SER measurements was evaluated by using the intraclass correlation coefficient.

Results: There were 15 of 215 (7.0%) IBTR cases (nine DCIS cases and six invasive cases) at a median of 36 months (range, 11–61 months). Multivariate analysis showed that higher parenchymal SER (hazard ratio [HR] = 2.028, $P < .001$ for reader 1; HR = 1.652, $P < .001$ for reader 2) and larger histologic tumor size (HR = 1.360, $P = .009$ for reader 1; HR = 1.402, $P = .006$ for reader 2) were independent factors associated with worse IBTR-free survival. The intraclass correlation coefficient of SER measurements between two readers was 0.852 (95% confidence interval: 0.811, 0.885).

Conclusion: Higher parenchymal SER around the tumor at preoperative dynamic contrast-enhanced MR imaging and larger histologic tumor size were independent factors associated with worse IBTR-free survival in patients with DCIS after breast conservation surgery.

[1] From the Department of Radiology, Seoul National University College of Medicine, Seoul National University Hospital, 101 Daehak-ro, Jongno-gu, Seoul 110-744, Republic of Korea. Received February 20, 2013; revision requested April 10; revision received July 5; accepted August 9; final version accepted August 14. Supported by the Korea Healthcare Technology R&D Project, Ministry of Health & Welfare, Republic of Korea (grant A102065-37). **Address correspondence to** N.C. (e-mail: *river7774@gmail.com*).

Along with the widespread use of screening mammography today, the diagnosis of ductal carcinoma in situ (DCIS) has seen a marked increase (1,2). Although DCIS has a high probability of long-term disease-free survival, the risk of ipsilateral breast tumor recurrence (IBTR) is approximately 10%–30% at 10 years after breast conservation surgery without adequate radiation or endocrine therapy, as suggested by the National Comprehensive Cancer Network guidelines (3–5). The National Institutes of Health State-of-the-Science Conference has yielded recommendations that in the future, researchers should look to improve risk stratification of patients with DCIS, thereby leading to more individualized therapy decisions and reducing the side effects of radiation or endocrine therapy (6). Thus far, patient age, menopausal status, family history, margin status, nuclear grade, and molecular subtype of the tumor have been reported to be factors associated with IBTR (3,6,7). Consequently, treatment of patients with DCIS is currently based mainly on these clinical-pathologic features. However, thus far, imaging markers to guide therapy decisions have been lacking.

Advances in Knowledge

- In women with ductal carcinoma in situ (DCIS), a higher parenchymal signal enhancement ratio (SER) around the tumor at preoperative dynamic contrast-enhanced MR imaging and larger histologic tumor size were independently associated with worse ipsilateral breast tumor recurrence (IBTR)–free survival at multivariate analysis.
- The parenchymal SER around the tumor at preoperative dynamic contrast-enhanced MR imaging was effective when distinguishing the subsequent IBTR and no-IBTR groups (area under the receiver operating characteristic curve [A_z] = 0.885, 95% confidence interval [CI]: 0.817, 0.952 [$P < .001$] for reader 1; and A_z = 0.766, 95% CI: 0.614, 0.917 [$P = .001$] for reader 2).

A number of preclinical studies have shown that normal-appearing tissue surrounding a tumor, or cancer-associated stroma, plays a role in the progression of breast cancer (8–11). Indeed, high mammographic breast density has been reported to be associated with subsequent breast cancer events in women with DCIS in the National Surgical Adjuvant Breast and Bowel Project B-17 trial, after adjusting for treatment with radiation therapy, age, and body mass index (12). The amount of background parenchymal enhancement at magnetic resonance (MR) imaging has also been reported to be associated with breast cancer risk in a screening population (13). In addition, parenchymal signal enhancement ratio (SER) around the tumor at dynamic contrast material–enhanced MR imaging has been shown to be associated with response to chemotherapy and disease-free survival in patients with invasive breast cancer (14).

However, although the association between background parenchymal SER and survival outcomes in patients with invasive breast cancers has been studied, no investigators, to our knowledge, have assessed this association in patients with DCIS who have undergone breast conservation surgery. Therefore, the purpose of this study was to retrospectively investigate whether the background parenchymal features around the tumor at preoperative dynamic contrast-enhanced MR imaging are associated with IBTR-free survival in patients with DCIS after breast conservation surgery.

Materials and Methods

Study Population

Our institutional review board approved this study; the requirement for informed consent was waived. Between January 2004 and December 2009, 320 women with a pathologic diagnosis of pure DCIS after curative surgery were retrospectively identified through a search of the preoperative breast MR imaging database at our institution. Among them, 88 women who had undergone total mastectomy, 12 women who had undergone preoperative MR examinations at an outside hospital, three women without available follow-up data of at least 2 years' duration (mammography, ultrasonography, or MR imaging), and two women who had a previous history of breast cancer were excluded. Finally, 215 consecutive women (median age, 47 years; range, 24–74 years) composed our study population. Five of the women had synchronous bilateral DCIS lesions, and 210 patients had a unilateral lesion. In the cases of women with bilateral cancers, images of the more dominant lesion were analyzed.

Clinical-pathologic Analysis

Age, menopausal status, presentation of clinical findings, and biopsy methods

Implication for Patient Care

- When a woman with DCIS shows lower parenchymal SER around a tumor at preoperative dynamic contrast-enhanced MR imaging and smaller size at histologic examination, radiation therapy or hormonal therapy may be avoided.

Published online before print
10.1148/radiol.13130459 **Content codes:** BR MR

Radiology 2014; 270:699–707

Abbreviations:
A_z = area under the ROC curve
BPE = background parenchymal enhancement
CI = confidence interval
DCIS = ductal carcinoma in situ
ER = estrogen receptor
HER-2 = human epidermal growth factor receptor 2
HR = hazard ratio
IBTR = ipsilateral breast tumor recurrence
ICC = intraclass correlation coefficient
PR = progesterone receptor
ROC = receiver operating characteristic
ROI = region of interest
SER = signal enhancement ratio

Author contributions:
Guarantors of integrity of entire study, S.A.K., N.C.; study concepts/study design or data acquisition or data analysis/interpretation, all authors; manuscript drafting or manuscript revision for important intellectual content, all authors; approval of final version of submitted manuscript, all authors; literature research, S.A.K., N.C., J.M.C.; clinical studies, S.A.K., N.C., M.S., M.S.B., J.M.C.; experimental studies, E.B.R.; statistical analysis, S.A.K., N.C.; and manuscript editing, S.A.K., N.C., J.M.C.

Conflicts of interest are listed at the end of this article.

were obtained from medical records. Histologic tumor size; nuclear grade; the expression status of the estrogen receptor (ER), progesterone receptor (PR), and human epidermal growth factor receptor 2 (HER-2); and margin status of the tumor were obtained from standardized histopathology reports. ER and PR positivity were defined as the presence of 10% or more positively stained nuclei at 10× magnification. The intensity of c-erbB-2 staining was scored as 0, 1+, 2+, or 3+. Tumors with a 3+ score were classified as HER-2 positive, and tumors with a 0 or 1+ score were classified as negative. In tumors with a 2+ score, gene amplification by using fluorescence in situ hybridization was used to determine HER-2 status. The ratios of HER-2 gene copies to the centromeric region of chromosome 17 that were less than 2.2 were interpreted as normal, and ratios of 2.2 and higher were interpreted as amplified (15). The immunohistochemical subtype of the tumor was classified as hormonal receptor positive (ER or PR positive), HER-2 enriched (ER negative, PR negative, or HER-2 positive), or triple negative (ER negative, PR negative, and HER-2 negative).

With regard to the surgical resection margin status, surgeons tried to attain at least a 1-cm safety margin width from the tumor boundary during breast conservation surgery. Preoperative image-guided needle localization for nonpalpable lesions and intraoperative frozen biopsy for resection margins of surgical specimens were performed routinely. Margin width was classified as positive, close (<2 mm), or negative. Immediate repeat excision was performed for patients with positive margins at frozen biopsy. Delayed repeat excision was performed for patients with positive margins in their permanent histology report. Patients with negative margins in the immediate or delayed repeat excision specimens were classified as having negative margins (7).

With regard to adjuvant therapy, ipsilateral whole-breast irradiation was offered to patients after breast conservation surgery. The prescription dose was 50 or 50.4 Gy, with a daily dose of 1.8–2.0 Gy. A tumor bed boost and regional node irradiation were not used. Twenty-one of 215 patients (9.8%) had not undergone radiation therapy for the following reasons: *(a)* the patient refused ($n = 10$), *(b)* the surgical specimen yielded a tumor diameter smaller than 1 cm ($n = 7$), or *(c)* the surgeon was confident in achieving a wide safety margin ($n = 4$). No patient underwent adjuvant systemic chemotherapy, including trastuzumab. Adjuvant endocrine therapy had been recommended for patients with hormone receptor–positive DCIS. Among 169 patients with hormone receptor–positive tumors, 12 patients (7.1%) did not undergo adjuvant endocrine therapy because of patient refusal.

MR Imaging Technique

All preoperative MR examinations were performed by using a 1.5-T MR imaging system (Signa; GE Medical Systems, Milwaukee, Wis) with a dedicated phased-array breast coil, with the patient in the prone position. After obtaining a transverse localizer image, sagittal fat-suppressed, T2-weighted, fast spin-echo images were obtained (repetition time msec/echo time msec, 5500–7150/82; 256 × 160 matrix; field of view, 200 × 200 mm; 1.5-mm section thickness; no gap). Dynamic contrast-enhanced MR examinations included one precontrast acquisition and five postcontrast bilateral sagittal acquisitions by using a fat-suppressed T1-weighted three-dimensional fast spoiled gradient-echo sequence (6.5/2.5; matrix, 256 × 160; flip angle, 10°; field of view, 200 × 200 mm; 1.5-mm section thickness; no gap). Gadobenate dimeglumine (Multihance; Bracco Imaging, Milan, Italy) was injected into an antecubital vein by using an automated injector (Spectris MR; Medrad Europe, Maastricht, the Netherlands) at a dose of 0.1 mmol per kilogram of body weight and at a rate of 2 mL/sec. This was followed by a 20-mL saline flush. The time between the start of contrast material injection and the start of the first postcontrast series was 15 seconds. Acquisition time of each postcontrast series was 76 seconds. Five postcontrast image series were obtained at 91, 180, 360, 449, and 598 seconds after the start of contrast material administration. The resulting temporal sampling of the center of k-space for the postcontrast series occurred at approximately 45, 90, 180, 225, and 299 seconds. For all studies, early subtraction (ie, first postcontrast images minus precontrast images), axial reformatted, and three-dimensional maximum-intensity projection images were generated. We did not use software to generate registered subtraction images, as motion artifact was minimal in breast MR imaging. The mean interval between the MR examination and surgery was 4.4 days (range, 1–29 days). MR imaging examinations were not scheduled according to the patient's menstrual cycle.

MR Image Analysis

For qualitative assessment, all MR images were assessed retrospectively by two radiologists in consensus (S.A.K and N.C., with 3 and 10 years of experience in interpreting breast MR images, respectively) by using a picture archiving and communication system workstation. The radiologists were made aware that the patients had a histopathologic diagnosis of DCIS but were blinded to the information regarding IBTR and histologic tumor size. The information on tumor location was provided to the reviewers for more consistent quantitative analyses. Lesion size was defined as the maximal diameter of the enhancing lesion conspicuously delineated on early postcontrast images (91 seconds after contrast material injection), with a contrast level of at least 50% enhancement compared with the signal intensity on precontrast images, which was the empirical threshold to discriminate a DCIS lesion from the normal parenchyma. Lesion type was classified as mass or nonmass enhancement. To assess lesion kinetics, the whole series of dynamic contrast-enhanced MR images was assessed, and a circular region of interest (ROI), 5 mm in diameter, was placed on the most enhancing portion on the first postcontrast series. The type of lesion kinetics was categorized as persistent, plateau, or washout on the basis of images obtained in the delayed enhancement phase (16). We could not analyze the size, lesion type, and enhancement kinetics of tumors in

the 57 patients (26.5% of total patients) who had undergone excisional biopsy. The level of background parenchymal enhancement (BPE) was categorized as minimal (<25% of glandular tissue demonstrating contrast enhancement), mild (25%–50% enhanced glandular tissue), moderate (51%–75% enhanced glandular tissue), or marked (>75% enhanced glandular tissue) on the basis of both the volume and intensity of enhancement by using a combination of nonenhanced and early postcontrast T1-weighted fat-suppressed images and subtraction images, as performed in previous studies (13,17). Small areas of very intense enhancement were described as moderate or marked when the volume requirement was not met (17). In addition, the radiologists assigned the level of BPE on a quantitative scale (as a percentage) volumetrically.

The amount of fibroglandular tissue was defined as any nonfatty noncystic breast parenchyma that appeared fatty (<25%), had scattered fibroglandular density (25%–50%), was heterogeneously dense (51%–75%), or was extremely dense (>75% of the breast comprised glandular tissue), on the basis of a combination of T2-weighted fat-suppressed imaging and nonenhanced T1-weighted fat-suppressed imaging (13).

The SER of normal-appearing parenchyma around the tumor was calculated on a representative sagittal section that showed the largest dimension of the tumor on early postcontrast images by using the following equation (14):

$$\mathrm{SER} = (S_e - S_p)/(S_d - S_p),$$

where S_p, S_e, and S_d represent the signal intensity on precontrast (before contrast material administration), early postcontrast (91 seconds after contrast material injection), and delayed postcontrast (598 seconds after contrast material injection) images, respectively. Five ROIs, each with a 5-mm diameter, were juxtaposed by one radiologist (S.A.K., with 3 years of experience in the interpretation of breast MR imaging), so that the ROIs extended radially from the tumor edge, with the first ROI within the margin of the enhancing tumor and the next four in the normal-appearing parenchyma extending radially 2 cm from the boundary of the tumor on early postcontrast images (Figure, part a). To evaluate intraobserver variability of SER measurements, the second set of these ROIs was placed along a different direction (Figure, part b). For measurements of S_p and S_d, ROIs on early postcontrast images were copied and pasted onto corresponding sections of precontrast and delayed postcontrast images (Figure, parts c and d). Mean SERs from the four ROIs in the normal-appearing parenchyma of each set were calculated. The reader acquired repeat SER measurements along a different direction, which were averaged and used for further analysis.

To evaluate interobserver variability for SER measurements, another radiologist (E.B.R., 2 years of experience interpreting breast MR images) independently measured the SER for all cases in a manner similar to the first radiologist. SER measurement data from two readers were entered separately into univariate and multivariate analyses.

Statistical Analysis

The primary outcome was IBTR-free survival. IBTR was defined as any recurrence of a tumor in the ipsilateral breast without evidence of simultaneous distant recurrence occurring within 4 months after the diagnosis of the first IBTR (18). IBTR-free survival was defined as the time from the date of surgery to the date of IBTR detection at follow-up imaging. Data in patients with no IBTR were collected at the date of most recent follow-up without evidence of disease. IBTR-free survival rates were calculated by using the Kaplan-Meier method. The log-rank test was used for univariate comparisons. A Cox proportional hazards model was used to analyze the hazard ratio (HR) with 95% confidence intervals (CIs) for IBTR-free survival with clinical-pathologic variables (age, menopausal status, clinical presentation, biopsy method, histologic tumor size, nuclear grade, ER status, immunohistochemical subtype, surgical margin status, adjuvant radiation therapy, and adjuvant endocrine therapy) and MR imaging parameters (lesion size, lesion type, lesion kinetics, BPE, fibroglandular tissue density, and background parenchymal SER). Changes in HR were calculated with a 0.1-unit difference in background parenchymal SER, a 1-cm difference in tumor size, and a 10% difference in quantitative BPE. Variables with *P* values less than .05 at univariate analysis were entered as input variables for the multivariate model. There were no cases with missing data, and all cases were included in the Cox model. For each covariate, the proportional hazards assumption was verified initially by means of graphic checks, by using a log-minus-log survival plot. Formal checks were derived from a test based on time-dependent covariates, and Cox-Snell residuals were used to evaluate the fit of the model. A plot of the estimated cumulative hazard rate versus Cox-Snell residuals followed a 45° line.

Pearson correlation was used to compare tumor size at MR imaging and tumor size measured at surgical histopathologic examination.

To evaluate the diagnostic performance of the independent variables associated with IBTR-free survival, empirical receiver operating characteristic (ROC) curve analysis was performed in distinguishing IBTR from non-IBTR groups. Reproducibility of SER measurements was evaluated by using intraclass correlation coefficients (ICCs). Inter- and intraobserver agreements were assessed by applying a two-way ICC with a random-raters assumption and a one-way ICC, respectively. Statistical analyses regarding background SER were performed independently for the values obtained by readers 1 and 2.

A two-sided significance level of 5% was used for all analyses. SPSS software (version 19.0; SPSS, Chicago, Ill) was used for all data analyses except the ROC curve analysis, which was performed by using MedCalc software (version 10.3.0.0; MedCalc Software, Mariakerke, Belgium).

Results

Patients and Survival Outcome

Most patients were premenopausal women (69.3%, 149 of 215) who received a diagnosis of DCIS because of

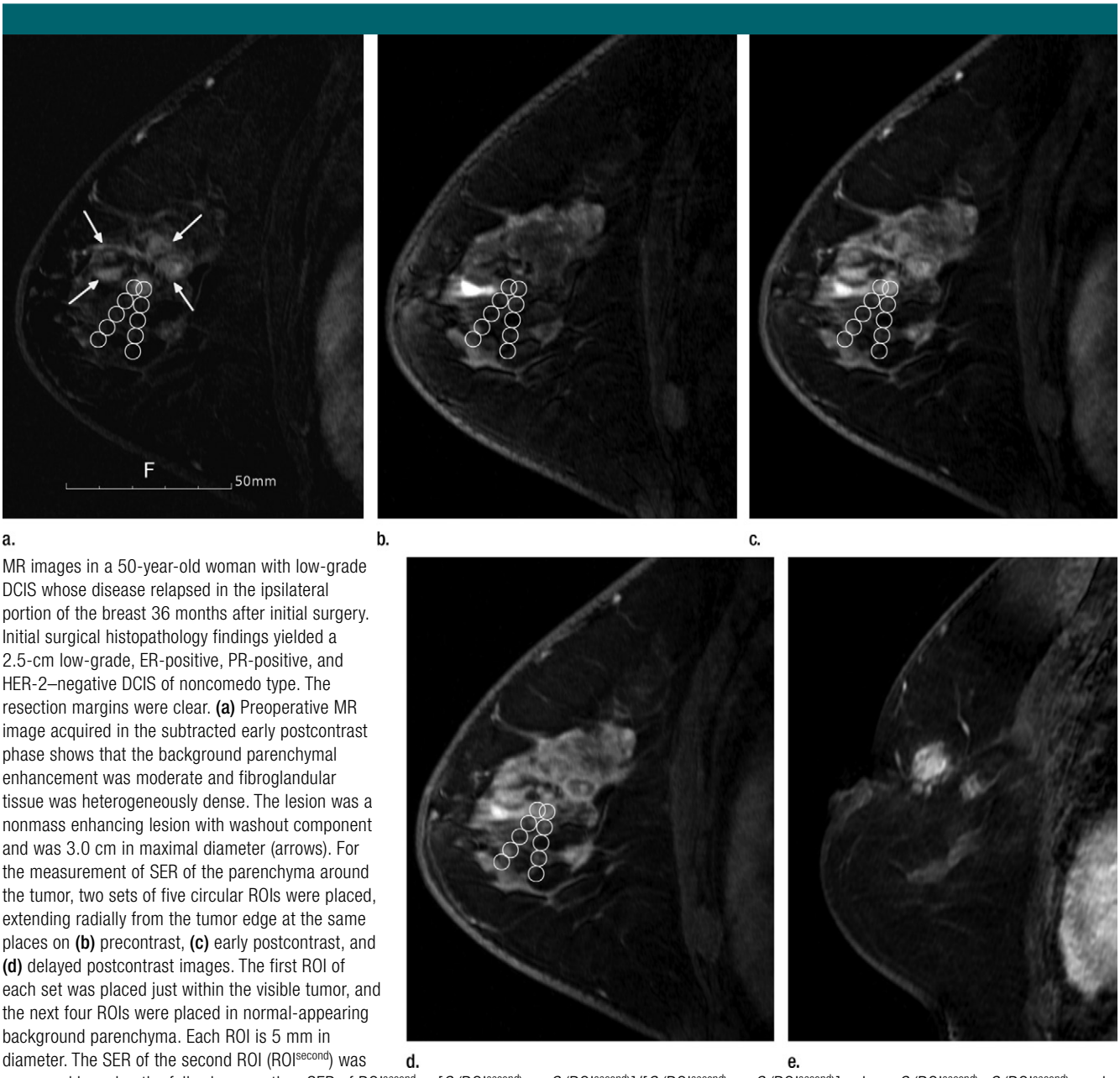

MR images in a 50-year-old woman with low-grade DCIS whose disease relapsed in the ipsilateral portion of the breast 36 months after initial surgery. Initial surgical histopathology findings yielded a 2.5-cm low-grade, ER-positive, PR-positive, and HER-2–negative DCIS of noncomedo type. The resection margins were clear. **(a)** Preoperative MR image acquired in the subtracted early postcontrast phase shows that the background parenchymal enhancement was moderate and fibroglandular tissue was heterogeneously dense. The lesion was a nonmass enhancing lesion with washout component and was 3.0 cm in maximal diameter (arrows). For the measurement of SER of the parenchyma around the tumor, two sets of five circular ROIs were placed, extending radially from the tumor edge at the same places on **(b)** precontrast, **(c)** early postcontrast, and **(d)** delayed postcontrast images. The first ROI of each set was placed just within the visible tumor, and the next four ROIs were placed in normal-appearing background parenchyma. Each ROI is 5 mm in diameter. The SER of the second ROI (ROI^{second}) was measured by using the following equation: SER of $ROI^{second} = [S_e(ROI^{second}) - S_p(ROI^{second})]/[S_d(ROI^{second}) - S_p(ROI^{second})]$, where $S_p(ROI^{second})$, $S_e(ROI^{second})$, and $S_d(ROI^{second})$ represent the signal intensity measured at the second ROI on the precontrast, early postcontrast, and delayed postcontrast images, respectively. The third, fourth, and fifth SERs were calculated by using the same equation. Thereafter, the mean value of SER from the four ROIs that were located in normal-appearing background parenchyma around the tumor was calculated. In this case, the mean SER of normal-appearing parenchyma around the tumor was 0.659. The patient did not undergo radiation therapy or endocrine therapy. Thirty-six months later, a mass was detected at screening mammography (not shown). **(e)** Early postcontrast MR image shows an irregularly enhancing mass in the remaining ipsilateral breast tissue. It was confirmed to be a 2.0-cm, ER-positive, PR-positive, HER-2–negative invasive ductal carcinoma of nuclear grade 2 and histologic grade II, associated with low-grade DCIS.

imaging abnormalities (75.3%, 162 of 215) and who underwent percutaneous core-needle biopsy (73.5%, 158 of 215) (Table 1). The mean tumor size at surgical histologic examination was 2.9 cm ± 2.0 (range, 0.2–9.8 cm). The correlation coefficient between the tumor size at MR imaging and the tumor size at surgical histologic evaluation was 0.533 ($P = .139$). In the IBTR group, the correlation coefficient was 0.614 ($P < .001$).

Table 1

Univariate Analysis between Variables and IBTR-free Survival Outcome

Variable	No. of Patients ($n = 215$)	No. of IBTRs ($n = 15$)	HR	95% CI	*P* Value
Age at surgery				0.598, 4.563	.328
<45 y	76 (35.3)	7 (46.7)	1.652		
≥45 y	139 (64.7)	8 (53.3)	1		
Menopause				0.669, 13.138	.133
Premenopause/perimenopause	149 (69.3)	13 (86.7)	2.964		
Postmenopause	66 (30.7)	2 (13.3)	1		
Presentation				0.806, 6.399	.121
Clinical	53 (24.6)	6 (40.0)	2.271		
Radiologic	162 (75.3)	9 (60.0)	1		
Biopsy method				0.877, 7.021	.087
Excision	57 (26.5)	6 (40.0)	2.481		
Core-needle biopsy	158 (73.5)	9 (60.0)	1		
Mean histologic tumor size (cm)*	2.9 ± 2.0	3.9 ± 2.1	1.270	1.016, 1.589	.036
Nuclear grade				0.493, 3.759	.549
Low	95 (44.2)	8 (53.3)	1.362		
Intermediate/high	120 (55.8)	7 (46.7)	1		
ER status				0.338, 3.351	.915
Positive	156 (72.6)	11 (73.3)	1.064		
Negative	59 (27.4)	4 (26.7)	1		
Immunohistochemical subtype					.830
Triple negative	23 (10.7)	2 (13.3)	1.356	0.301, 6.104	
HER-2 enriched	23 (10.7)	1 (6.7)	0.650	0.085, 5.005	
Hormone receptor positive	169 (78.6)	12 (80.0)	1		
Surgical margin status				0.753, 6.451	.139
Close (<2 mm)	39 (18.1)	5 (33.3)	2.204		
Negative	176 (81.9)	10 (66.7)	1		
Radiation therapy				1.092, 10.938	.025
No	21 (9.8)	4 (26.7)	3.455		
Yes	194 (90.2)	11 (73.3)	1		
Endocrine therapy				1.347, 10.327	.007
No	56 (26.0)	8 (53.3)	3.730		
Yes	159 (74.0)	7 (46.7)	1		
Mean lesion size at MR imaging (cm)*†	2.8 ± 1.8	2.4 ± 1.1	0.875	0.570, 1.343	.541
Lesion type ($n = 158$)†				0.344, 8.039	.523
Mass	21 (13.3)	2 (22.2)	1.663		
Nonmass-like enhancement	137 (86.7)	7 (77.8)	1		
Lesion kinetics ($n = 158$)†				1.218, 16.927	.013
Washout and plateau‡	34 (21.6)	5 (55.6)	4.541		
Persistent	124 (78.5)	4 (44.4)	1		
Qualitative BPE§				0.632, 5.447	.254
Marked	45 (20.9)	6 (40.0)	1.855		
Moderate	60 (27.9)	4 (26.7)			
Mild	74 (34.4)	4 (26.7)	1		
Minimal	36 (16.7)	1 (6.7)			
Mean quantitative BPE (%)*	39.8 ± 30.2	51.2 ± 28.9	1.121	0.937, 1.342	.210
Fibroglandular tissue density§				0.517, 10.237	.261
Extremely dense	82 (38.1)	7 (46.7)	2.300		
Heterogeneously dense	81 (37.7)	6 (40.0)			
Scattered fibroglandular tissue	47 (21.9)	2 (13.3)	1		
Fatty	5 (2.3)	0 (0.0)			

Table1 (continues)

Table 1 (continued)

Univariate Analysis between Variables and IBTR-free Survival Outcome

Variable	No. of Patients (n = 215)	No. of IBTRs (n = 15)	HR	95% CI	P Value
Mean parenchymal SER*					
Reader 1	0.352 ± 0.152	0.574 ± 0.142	2.109	1.574, 2.824	<.001
Reader 2	0.336 ± 0.161	0.533 ± 0.241	1.690	1.331, 2.146	<.001

Note.—Values in parentheses are percentages.

* Data are means ± standard deviations.

† Data were obtained in patients who had not undergone excisional biopsy before MR examination. Among those patients, nine experienced IBTR.

‡ Washout and plateau patterns were combined for the analysis of HR, CIs, and P values.

§ The lower two categories and upper two categories of the four-point scales of BPE and fibroglandular tissue density were combined for the analysis of HR, CIs, and P values.

IBTR occurred in 15 patients (7.0%, 15 of 215) at a median of 36 months (range, 11–61 months). Forty percent of patients (six of 15) developed invasive recurrent cancers, and 60.0% (nine of 15) developed DCIS. Twenty percent of IBTRs (three of 15) occurred at the surgical scar sites of initial cancers, and 80% of IBTRs (12 of 15) occurred at different quadrants. In addition, 53% of recurrent cancers (eight of 15) occurred in patients who had low-grade DCIS. No women developed metastasis or death-related breast cancer. The remaining 200 patients did not experience IBTR at a median of 48 months (range, 27–100 months) of follow-up.

Survival Analysis: Univariate

A higher background parenchymal SER around the tumor (HR = 2.109, 95% CI: 1.574, 2.824 [$P < .001$] for reader 1; HR = 1.690, 95% CI: 1.331, 2.146 [$P < .001$] for reader 2), omission of endocrine therapy (HR = 3.730; 95% CI: 1.347, 10.327 [$P = .007$]), omission of radiation therapy (HR = 3.455, 95% CI: 1.092, 10.938 [$P = .025$]), plateau or washout kinetic pattern of tumor at MR imaging (HR = 4.541, 95% CI: 1.218, 16.927 [$P = .013$]), and larger tumor size at histologic examination (HR = 1.270, 95% CI: 1.016, 1.589 [$P = .036$]) were significantly associated with worse IBTR-free survival at univariate analysis (Table 1).

There were no significant associations between IBTR-free survival outcome and age ($P = .328$), menopausal status ($P = .133$), initial presentation ($P = .121$), biopsy method ($P = .087$), nuclear grade ($P = .549$), ER status ($P = .915$), immunohistochemical subtype ($P = .830$), surgical margin status ($P = .139$), lesion size at MR imaging ($P = .541$), lesion type (mass vs nonmass-like enhancement) ($P = .523$), qualitative BPE ($P = .254$), quantitative BPE ($P = .210$), and amount of fibroglandular tissue ($P = .261$) (Table 1).

Survival Analysis: Multivariate

Variables showing a P value of less than .05 at univariate analyses, including parenchymal SER around the tumor, tumor size at histologic examination, status of endocrine therapy, and status of radiation therapy, were entered as input variables for multivariate analysis.

Multivariate analysis showed that higher parenchymal SER around the tumor (HR = 2.028, 95% CI: 1.505, 2.731 [$P < .001$] for reader 1; HR = 1.652, 95% CI: 1.302, 2.095 [$P < .001$] for reader 2) and larger histologic tumor size (HR = 1.360, 95% CI: 1.080, 1.713 [$P = .009$] for reader 1; HR = 1.402, 95% CI: 1.100, 1.786 [$P = .006$] for reader 2) remained independent variables associated with worse recurrence-free survival (Table 2) (Figure).

ROC Analysis in Distinguishing IBTR from Non-IBTR Groups

The area under the ROC curve (A_z) for the mean SER around the tumor obtained by reader 1 and reader 2 was 0.885 (95% CI: 0.817, 0.952; $P < .001$) and 0.766 (95% CI: 0.614, 0.917; $P = .001$) in distinguishing IBTR from non-IBTR groups. The A_z of the histologic tumor size was 0.670 (95% CI: 0.552, 0.789; $P = .028$) in distinguishing IBTR from non-IBTR groups.

Intra- and Interobserver Variability for SER Measurements

The ICC values between repeated measurements of mean SER along different directions (intraobserver variability) for readers 1 and 2 were 0.889 (95% CI: 0.857, 0.914; $P < .001$) and 0.875 (95% CI: 0.839, 0.903; $P < .001$), respectively, which indicates excellent agreement. ICC between the two readers (interobserver variability) was 0.852 (95% CI: 0.811, 0.885; $P < .001$), which also indicates excellent agreement.

Discussion

We found that higher parenchymal SER around the tumor (HR = 2.028, 95% CI: 1.505, 2.731 [$P < .001$] for reader 1; HR = 1.652, 95% CI: 1.302, 2.095 [$P < .001$] for reader 2) at preoperative MR imaging and larger histologic tumor size (HR = 1.360, 95% CI: 1.080, 1.713 [$P = .009$] for reader 1; HR = 1.402, 95% CI: 1.100, 1.786 [$P = .006$] for reader 2) were independent variables associated with worse IBTR-free survival in patients with DCIS who had been treated with breast conservation surgery after controlling for adjuvant radiation therapy and endocrine therapy.

Quantification of SER at dynamic contrast-enhanced MR imaging is a practical alternative to the measurement

Table 2

Multivariate Cox Proportional Hazards Analysis of IBTR-free Survival Outcome

	HR		*P* Value	
Variable	Reader 1	Reader 2	Reader 1	Reader 2
Histologic tumor size	1.360 (1.080, 1.713)	1.402 (1.100, 1.786)	.009	.006
Parenchymal SER	2.028 (1.505, 2.731)	1.652 (1.302, 2.095)	<.001	<.001
Radiation therapy				
No	2.831 (0.841, 9.532)	3.004 (0.887, 10.173)	.093	.077
Yes	1	1		
Endocrine therapy				
No	2.629 (0.878, 7.869)	2.785 (0.951, 8.155)	.084	.062
Yes	1	1		

Note.—Numbers in parentheses are 95% CIs.

of k_{ep}, the rate constant for transport from extravascular space to plasma on the basis of a two-compartment pharmacokinetic model (19). It had been studied previously to characterize the vasculature of breast cancer itself for the prediction of recurrence (20). In our study, however, we applied this method to evaluate the normal-appearing parenchyma around the DCIS.

The association between higher SER around the tumor and IBTR can be explained by the role of a patient's stroma, which is permissive to the regrowth of tumors, even without residual DCIS. For the transition of DCIS to invasive ductal carcinoma, a study that involved a xenograft model of human DCIS validated the premise that normal myoepithelial cells suppressed tumor growth and progression, whereas stromal fibroblasts promoted progression to invasion via enhancing angiogenesis or increased endothelial permeability, leading to diffusion of gadolinium-based contrast agent out of leaky duct basement membranes (21,22). Indeed, in our study, although all patients had pure DCIS initially, 40% of patients (six of 15) developed invasive recurrent cancers. Another study reported that increased percentage of enhancement at dynamic contrast-enhanced MR imaging in normal breast tissue surrounding invasive breast cancer, within 2 cm of the tumor edge, was correlated with increased microvessel density and genomic changes through topographic mapping (23). Integrating our results with those of previous studies, we can infer that higher SER around the tumor at dynamic contrast-enhanced MR imaging shows potential as a noninvasive indicator of an otherwise occult, microscopic, residual DCIS focus or a stroma that is permissive to cancer progression and leads to subsequent IBTR.

As for tumor features, plateau or washout pattern of enhancement kinetics was associated with worse recurrence-free survival at univariate analysis ($P = .013$) in our study. This factor was not included in multivariate analysis, as we could not analyze the enhancement kinetics of tumors in the 57 patients (26.5% of total patients) who had undergone excisional biopsy. To date, there has been limited data regarding the association between enhancement kinetics of DCIS and IBTR. With regard to invasive cancers, the washout enhancement kinetic pattern has been reported to correlate with high histologic grade, high Ki-67 expression, and increased vascular permeability, suggesting an aggressive tumor (24,25). Pure DCIS lesions are known to show a variety of kinetic curve patterns, including persistent, plateau, and washout types. Contrary to our results, there has been no definite association between enhancement kinetic features and nuclear grade of DCIS (26).

Our study has some limitations. First, this is a retrospective study from a single institution, and the sample size was small. As we included a small number of IBTR ($n = 15$) cases with 16 variables in univariate analysis, there is a possibility of type-I error, owing to multiple statistical testing from a small sample size. However, the significant variables, including histologic tumor size and status of endocrine therapy or radiation therapy, have been constantly reported to be related to IBTR in previous studies. Regarding the parenchymal SER, since the *P* value of parenchymal SER at multivariate analysis was less than .001, we believe it would have been sufficiently significant even after corrections for multiple testing, and the possibility of type-I error would be very low. Second, measurement of parenchymal SER around the tumor may be somewhat subjective, as selection of a representative image and placement of ROIs might have affected the results. However, ICC values of repeated measurements along different directions by two readers (intraobserver variability, 0.889 and 0.875) and that between the two readers (interobserver variability, 0.852) indicated excellent agreement. An objective method for SER quantification, such as computer-aided SER mapping, should be considered in future studies. Third, MR imaging examinations were not scheduled according to the women's menstrual cycles, which could have affected the results. According to a recent study, the amount of BPE differed significantly between weeks 2 and 4 but not between other weeks of the menstrual cycle, and the degree of BPE was significantly weaker in weeks 1 and 2 than in weeks 3 and 4 (27). Although scheduling of screening MR imaging in the second week of a woman's menstrual cycle is routinely recommended to minimize the issue of background parenchymal enhancement, diagnostic MR imaging for staging of breast cancer is usually performed, regardless of the menstrual cycle, in clinical practice (17). Consideration of the menstrual cycle may need to be a routine part of breast MR examinations, as evidence seems to be mounting for its effect on BPE.

In conclusion, higher background parenchymal SER around the tumor

at preoperative MR imaging and larger histologic tumor size were independent significant factors associated with worse IBTR-free survival in patients with DCIS who underwent breast conservation surgery. Thus, in the future, when a patient with breast DCIS shows a lower parenchymal SER around a tumor at preoperative dynamic contrast-enhanced MR imaging and smaller size at histologic examination, after confirmation of our results, it may be that radiation therapy or hormonal therapy may be avoided. On the basis of our observations, SER quantification around the tumor at preoperative dynamic contrast-enhanced MR imaging has the potential to serve as an additional tool for the risk stratification of patients with DCIS who are considering breast conservation surgery.

Disclosures of Conflicts of Interest: S.A.K. No relevant conflicts of interest to disclose. **N.C.** No relevant conflicts of interest to disclose. **E.B.R.** No relevant conflicts of interest to disclose. **M.S.** No relevant conflicts of interest to disclose. **M.S.B.** No relevant conflicts of interest to disclose. **J.M.C.** No relevant conflicts of interest to disclose. **W.K.M.** No relevant conflicts of interest to disclose.

References

1. Kuerer HM, Albarracin CT, Yang WT, et al. Ductal carcinoma in situ: state of the science and roadmap to advance the field. J Clin Oncol 2009;27(2):279–288.
2. Virnig BA, Tuttle TM, Shamliyan T, Kane RL. Ductal carcinoma in situ of the breast: a systematic review of incidence, treatment, and outcomes. J Natl Cancer Inst 2010;102(3):170–178.
3. EORTC Breast Cancer Cooperative Group; EORTC Radiotherapy Group, Bijker N, et al. Breast-conserving treatment with or without radiotherapy in ductal carcinoma-in-situ: ten-year results of European Organisation for Research and Treatment of Cancer randomized phase III trial 10853—a study by the EORTC Breast Cancer Cooperative Group and EORTC Radiotherapy Group. J Clin Oncol 2006;24(21):3381–3387.
4. Holmberg L, Garmo H, Granstrand B, et al. Absolute risk reductions for local recurrence after postoperative radiotherapy after sector resection for ductal carcinoma in situ of the breast. J Clin Oncol 2008;26(8):1247–1252.
5. NCCN guidelines for breast cancer. http://www.nccn.com/files/cancer-guidelines/breast/index.html. Published DATE. Accessed June 18, 2013.
6. Allegra CJ, Aberle DR, Ganschow P, et al. National Institutes of Health State-of-the-Science Conference statement: Diagnosis and Management of Ductal Carcinoma in Situ September 22-24, 2009. J Natl Cancer Inst 2010;102(3):161–169.
7. Rudloff U, Jacks LM, Goldberg JI, et al. Nomogram for predicting the risk of local recurrence after breast-conserving surgery for ductal carcinoma in situ. J Clin Oncol 2010;28(23):3762–3769.
8. Friedl P, Alexander S. Cancer invasion and the microenvironment: plasticity and reciprocity. Cell 2011;147(5):992–1009.
9. Cichon MA, Degnim AC, Visscher DW, Radisky DC. Microenvironmental influences that drive progression from benign breast disease to invasive breast cancer. J Mammary Gland Biol Neoplasia 2010;15(4):389–397.
10. Heaphy CM, Griffith JK, Bisoffi M. Mammary field cancerization: molecular evidence and clinical importance. Breast Cancer Res Treat 2009;118(2):229–239.
11. Li Z, Moore DH, Meng ZH, Ljung BM, Gray JW, Dairkee SH. Increased risk of local recurrence is associated with allelic loss in normal lobules of breast cancer patients. Cancer Res 2002;62(4):1000–1003.
12. Habel LA, Dignam JJ, Land SR, Salane M, Capra AM, Julian TB. Mammographic density and breast cancer after ductal carcinoma in situ. J Natl Cancer Inst 2004;96(19):1467–1472.
13. King V, Brooks JD, Bernstein JL, Reiner AS, Pike MC, Morris EA. Background parenchymal enhancement at breast MR imaging and breast cancer risk. Radiology 2011;260(1):50–60.
14. Hattangadi J, Park C, Rembert J, et al. Breast stromal enhancement on MRI is associated with response to neoadjuvant chemotherapy. AJR Am J Roentgenol 2008;190(6):1630–1636.
15. Dolan M, Snover D. Comparison of immunohistochemical and fluorescence in situ hybridization assessment of HER-2 status in routine practice. Am J Clin Pathol 2005;123(5):766–770.
16. American College of Radiology. Breast imaging reporting and data system (BI-RADS)—MRI. Reston, Va: American College of Radiology, 2003.
17. Morris EA. Diagnostic breast MR imaging: current status and future directions. Radiol Clin North Am 2007;45(5):863–880, vii.
18. Taghian A, Jeong JH, Mamounas E, et al. Patterns of locoregional failure in patients with operable breast cancer treated by mastectomy and adjuvant chemotherapy with or without tamoxifen and without radiotherapy: results from five National Surgical Adjuvant Breast and Bowel Project randomized clinical trials. J Clin Oncol 2004;22(21):4247–4254.
19. Li KL, Henry RG, Wilmes LJ, et al. Kinetic assessment of breast tumors using high spatial resolution signal enhancement ratio (SER) imaging. Magn Reson Med 2007;58(3):572–581.
20. Li KL, Partridge SC, Joe BN, et al. Invasive breast cancer: predicting disease recurrence by using high-spatial-resolution signal enhancement ratio imaging. Radiology 2008;248(1):79–87.
21. Jansen SA, Paunesku T, Fan X, et al. Ductal carcinoma in situ: x-ray fluorescence microscopy and dynamic contrast-enhanced MR imaging reveals gadolinium uptake within neoplastic mammary ducts in a murine model. Radiology 2009;253(2):399–406.
22. Hu M, Yao J, Carroll DK, et al. Regulation of in situ to invasive breast carcinoma transition. Cancer Cell 2008;13(5):394–406.
23. Nabavizadeh N, Klifa C, Newitt D, et al. Topographic enhancement mapping of the cancer-associated breast stroma using breast MRI. Integr Biol (Camb) 2011;3(4):490–496.
24. Su MY, Cheung YC, Fruehauf JP, et al. Correlation of dynamic contrast enhancement MRI parameters with microvessel density and VEGF for assessment of angiogenesis in breast cancer. J Magn Reson Imaging 2003;18(4):467–477.
25. Lee SH, Cho N, Kim SJ, et al. Correlation between high resolution dynamic MR features and prognostic factors in breast cancer. Korean J Radiol 2008;9(1):10–18.
26. Rahbar H, Partridge SC, Demartini WB, et al. In vivo assessment of ductal carcinoma in situ grade: a model incorporating dynamic contrast-enhanced and diffusion-weighted breast MR imaging parameters. Radiology 2012;263(2):374–382.
27. Kajihara M, Goto M, Hirayama Y, et al. Effect of the menstrual cycle on background parenchymal enhancement in breast MR imaging. Magn Reson Med Sci 2013;12(1):39–45.